

## Removal of boron, fluoride and nitrate by electro dialysis in the presence of organic matter

Laura J. Banasiak and Andrea I. Schäfer

School of Engineering and Electronics, The University of Edinburgh, Edinburgh, EH9 3JL, United Kingdom

Ph: +44 (0) 131 650 7209; Fax: +44 (0) 131 650 6781; Email: Andrea.Schaefer@ed.ac.uk

### Abstract

*The removal of the trace inorganic contaminants boron ( $B(OH)_4^-$ ), fluoride ( $F^-$ ) and nitrate ( $NO_3^-$ ) from synthetic aqueous solutions containing organic matter using electro dialysis was investigated. The transport of the contaminants through the ion-exchange membranes was evaluated in relation to hydrated ionic radius, whereby a positive correlation was found in absence of organic matter.  $NO_3^-$ , with the smaller hydrated ionic radius and weaker hydration shell, was removed more effectively than  $F^-$ , which has a larger hydrated ionic radius and stronger hydration shell. The removal of  $F^-$  and  $NO_3^-$  was not significantly influenced by solution pH due to their pH independent speciation. However, the removal of boron was dependent on increasing solution pH and the degree of demineralization. Dissolved organic matter (humic acid, tannic acid and alginate) resulted in enhanced removal of boron and  $F^-$  as a result of the binding of  $F^-$  within the organic matter structure and complexation of boric acid ( $B(OH)_3$ ) with carboxylate groups in the organic matter. Deposition of organic matter to the anion-exchange membranes was noted. Inorganic trace contaminant and organic matter membrane deposition influenced system performance in regards to an increase in stack resistance and decrease in removal and flux of total dissolved solids.*

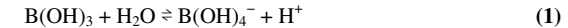
*Keywords: Electro dialysis; Ion transport; Inorganic trace contaminant removal; Dissolved organic matter; Fouling; Groundwater/Brackish water*

### 1. Introduction

Membrane processes such as electro dialysis (ED) are increasingly being utilised in water treatment to remove dissolved contaminants. A wide range of inorganic trace contaminants, including fluoride ( $F^-$ ) and nitrate ( $NO_3^-$ ), can be found in surface, brackish and groundwater. The occurrence and fate of these contaminants is an environmental and public health concern. Concentrations of  $F^-$  in surface water are relatively low (<0.1–0.5 mg/L) [1], while concentrations up to 20 mg/L have been found in groundwater [2]. The harmful effects of excess  $F^-$  (dental and skeletal fluorosis) have been widely studied [3, 4].  $NO_3^-$  concentrations in surface and groundwater have increased worldwide due to heavy utilization of artificial fertilizers [5]. Deleterious health effects due to  $NO_3^-$  include infantile methemoglobinemia (known as ‘blue-baby’ syndrome) and cancer risks for adults and older children [5]. According to the World Health Organization (WHO) [1], the European Union (EU) Drinking Water Directive [6] and the Australian Drinking Water Guidelines (ADWG) [7], the maximum levels for  $F^-$  and  $NO_3^-$  in drinking water are 1.5 and 50 mg/L, respectively. However, for  $NO_3^-$  a level of 25 mg/L has been recommended [1, 7]. Due to its high selectivity and low chemical demand, ED has proved an efficient method for desalination and the removal of  $F^-$  and  $NO_3^-$  [8, 9].

Boron is another contaminant of interest due to its occurrence in seawater and difficulty of removal in desalination. While natural concentrations in surface and groundwaters are usually low, concentrations up to 100 mg/L have been found as a result of wastewater discharge [10]. Long-term consumption of water and food products with increased boron content results in malfunctioning of cardiac-vascular, nervous, and alimentary systems of humans [11]. The WHO

and EU Council have set limits of 0.5 mg/L and 1 mg/L for drinking water, respectively [1, 6]. Boron removal using ED has previously been studied [12, 13]; however its interaction with organic matter (OM) and the subsequent impact on its removal has not been investigated. ED is capable of removing 42 – 75 % of boron, with removal efficiency dependent on solution pH (97 % at pH 9 – 10) and the degree of desalination [10, 13]. In acidic and near neutral aqueous environments boron is mainly present as  $B(OH)_3$  and partially as borate ions according to the dissociation reaction ( $K_a = 6 \times 10^{-10}$ ,  $pK_a$  9.24 at 25°C) [14]:



Organic matter (OM) occurs in aquatic ecosystems in concentrations of 0.5 to 100 mgC/L [15] and have been a focal point in water treatment research as they are precursors to disinfection by-products. Dissolved organic substances (e.g. humic substances) act as ligands for metal ions, oxides hydroxides, minerals and organic micropollutants and form water-soluble and water-insoluble complexes [16]. Organic matter comes with seasonal and location (origin) specific characteristics and hence it is important to consider diverse groups such as humics, polyphenols, and polysaccharides.

In ED, organic substances, such as humate, deposit on the ion-exchange membranes and can cause increases in electrical resistance of the membranes [17]. HA in particular has been reported to be responsible for fouling in ED which affects salt flux [18-20]. As most OM is negatively charged at neutral pH, deposits form predominantly on the anion exchange membranes. The impact of such deposits on removal of specific contaminants is not well understood. Further, solute-solute interactions (such as complexation) of OM with inorganic compounds ( $B(OH)_4^-$ ,  $F^-$  and  $NO_3^-$ ) has to date not been investigated. As such interactions are likely to affect removal, the main objective of this study was to examine the influence of pH and three types of OM on the removal of  $B(OH)_4^-$ ,  $F^-$  and  $NO_3^-$  during ED systematically. In order to achieve this goal the project was conducted in five stages, namely (1) mechanisms of inorganics removal (in absence of OM), (2) OM removal, (3) impact of OM on inorganics removal, (4) inorganic membrane deposit formation, and (5) organic deposit formation.

### 2. Materials and Methods

#### 2.1. Chemicals and solution preparation

The feed solution (dilute and concentrate, 4L each) was prepared by dissolving ACS reagent grade NaCl (5 g/L) and  $NaHCO_3$  (84 mg/L) (Fisher Scientific UK), NaF (5 mg/L; total mass 2.1 mmol),  $NaNO_3$  (100 mg/L; total mass 57 mmol) and  $H_3BO_3$  (10 mg/L; total mass 7.4 mmol) (Sigma Aldrich UK) in ultrapure water. The concentrations of  $H_3BO_3$ ,  $F^-$  and  $NO_3^-$  were selected within the range found in brackish waters [12, 21]. Experiments with an identical concentration of 10 mg/L for  $H_3BO_3$ ,  $F^-$  and  $NO_3^-$  as well as detailed investigation of the pH range 8.5 to 9.5 for the initial NaCl concentrations of 5 g/L and 20 g/L (results not shown). Data on hydrated ionic radii and hydration energy are outlined in Table 1.

Table 1: Characteristics of the ions.

Parameter	Unit	Na <sup>+</sup>	Cl <sup>-</sup>	F <sup>-</sup>	NO <sub>3</sub> <sup>-</sup>	B(OH) <sub>4</sub> <sup>-</sup>	References
Crystal ionic radii, <i>r</i>	nm	-	-	0.116 - 0.119	0.179 - 0.189	0.244-0.261	[30, 31, 43-46]
		0.117	0.164	0.133 - 0.135	0.206		[45, 47]
Hydrated ionic radii, $\Delta r$	nm	0.358	0.332	0.352	0.340	<sup>a</sup>	[31]
Number of water molecules in hydration shell, <i>n</i>	-	3.5	2.0	2.7	2.0	<sup>a</sup>	[47]
Molar Gibbs energy of hydration, $\Delta_{\text{hyd}} G_{\text{calc}}^{\circ}$	kJ/mol	-385	-270	-345	-275	<sup>a</sup>	[47]
Ion mobility at 25°C, <i>u</i>	m <sup>2</sup> /sV	5.19	7.91	5.70	7.40	<sup>a</sup>	[33]
Ion equivalent conductivity, $\lambda^{\circ}$ equiv	cm <sup>2</sup> /Ωequiv	50.1	76.4	55.4	71.5	<sup>a</sup>	[48]

<sup>a</sup>Data not available.

Na<sub>2</sub>SO<sub>4</sub> (99 % purity) was used in the electrode rinse solution (Fisher Scientific UK) and analytical grade reagents NaOH and HCl (Fisher Scientific UK) were used for pH adjustments and membrane cleaning.

Three different types of OM were selected for use in this study: humic acid sodium salt (HA), tannic acid (TA) and alginic acid sodium salt (AA) (all Sigma Aldrich UK). The concentration of OM in different waters is highly variable [15] and hence an average OM concentration of 12.5 mgC/L was used in all experiments. The respective OM solutions were prepared by dissolving HA, TA and AA in ultrapure water and adding them to the feed solution. Physical and chemical properties of the OM compounds are outlined in Table 2.

Major functional groups of HA include carboxylic, phenolic, alcohol/aldehyde acids, and methoxyl and HA is negatively charged at neutral pH [22]. As a polyphenol, TA can form inter- and intramolecular hydrogen bonds and often exists in solution as loosely bound complexes of molecules [23]. At acidic pH TA is neutrally charged, however as pH increases the charge becomes negative [24]. AA is a naturally occurring hydrophilic colloidal polysaccharide, is obtained from brown seaweed and exhibits negatively charged carboxylate and neutral hydroxyl groups at pH 7 [25]. Below pH 4, the charge density decreases causing increased aggregation, whereas above pH 8 dissociation has been observed [26].

Table 2: Physical and chemical properties of organic matter (OM).

Organic Type	Category	Origin	Molecular Formulae	MW (g/mol)	Carbon (%)	pKa	Acidic pH	Neutral pH	Basic pH	References
Humic Acid (HA)	OM surrogate	Soil	C <sub>342</sub> H <sub>388</sub> O <sub>124</sub> N <sub>5</sub> <sup>a</sup>	4100	56	3.5-5.04	Neutral	Negative	Negative	[22, 34, 41, 49-52]
Tannic Acid (TA)	Polyphenol	Plants	C <sub>76</sub> H <sub>52</sub> O <sub>46</sub>	1701	54	2.5-10	Neutral	Negative	Negative	[23]
Alginic Acid (AA)	Polysaccharide	Brown seaweed and algae	[C <sub>6</sub> H <sub>8</sub> O <sub>6</sub> ] <sub>n</sub>	21000	36	2.0-3.5	Negative	Negative	Negative	[26]

<sup>a</sup> Based on model by [53]. <sup>b</sup> Sigma Aldrich Humic Acid.

## 2.2. Electrodialysis System

The ED stack used was a BEL-500 unit (Berghof, Germany) with seven Neosepta CMX-SB cation-exchange membranes (CEMs) and six Neosepta AMX-SB anion-exchange membranes (AEMs) (supplied by Eurodia, Germany; manufactured by Astom Corporation, Tokyo, Japan) with an available membrane area of 58 cm<sup>2</sup> each. The ED cell was connected to a DC electric potential (GW Instek DC Power supply Model GPR-1810HD, Taiwan) through TiO<sub>2</sub>-coated titanium electrodes. A schematic of the ED system is shown in Figure 1.

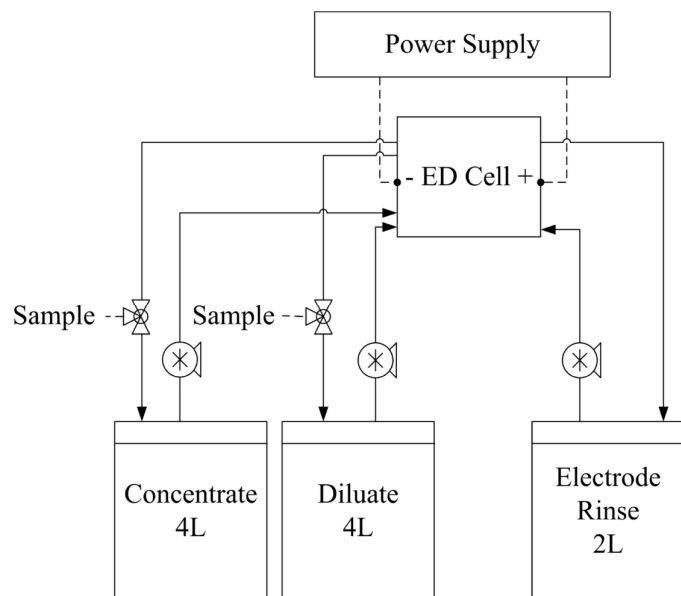


Figure 1. Schematic of the ED system used in this study

The limiting current density (LCD, 7.8 mA/cm<sup>2</sup>) was derived from a set of current-voltage curves measured in the ED cell and in consequence the applied voltage fixed to 10V to operate below the LCD. Diluate and concentrate were recirculated through the ED cell at a flow rate of 1.5 L/min until the desired product concentration (0.5 g/L NaCl) was achieved in the diluate. 0.5 mol/L Na<sub>2</sub>SO<sub>4</sub> was used as an electrode rinse solution at a flow rate of 1.5 L/min, in order to prevent the generation of chlorine or hypochlorite, which could be hazardous for the electrodes, had NaCl been used instead.

The resistance across the ED stack was calculated using Ohms law:

$$R = \frac{E}{I} \quad (2)$$

Where,  $R$  is the resistance (Ohm),  $E$  the electrical potential (Volt) and  $I$  the electrical current (Ampere).

## 2.3. Analytical Methods

The pH, electrical conductivity (EC) and temperature of samples taken from the diluate and concentrate during each experiment was measured using a pH/Conductivity meter (Multiline P4 combination pH electrode, WTW Germany).

F<sup>-</sup> and NO<sub>3</sub><sup>-</sup> concentrations were determined using ion-selective electrodes (ISE) in conjunction with a standard reference electrode connected to a Metrohm 781 Ion Meter (UK). The ISEs were regularly calibrated, with and without OM, and cleaned using standard methods. Standards and samples were mixed with a total ionic strength adjustment buffer (TISAB) to avoid possible interferences resulting from changes in solution pH and conductivity. NO<sub>3</sub><sup>-</sup> sample analysis was checked using a Quickchem 8500 FIA Nutrient Analyser (Lachat Instruments, Colorado, USA) and F<sup>-</sup> analysis was verified using a DX-500 ion chromatograph (DIONEX, Sunnyvale, CA, USA). Sample concentrations were in agreement with ISE results. Total concentrations of H<sub>3</sub>BO<sub>3</sub> were determined by ICP-OES using a Perkin Elmer Optima 5300DV instrument (Perkin Elmer, UK).

UV-Visible Spectrometry (Varian Cary 100 Scan, UK) was utilized to determine the absorbance of OM in experimental samples. HA was analyzed at a wavelength of 254 nm, whereas TA and AA were analyzed at wavelengths of 275 nm and 198 nm, respectively. Specific UV absorbance (SUVA, L/mg.m) values were calculated for HA as in eqn (3):

$$SUVA = \frac{UV\ Abs(m)}{DOC(mgC/L)} \times 100 \quad (3)$$

Non-purgeable organic carbon (NPOC) concentrations were determined using a total organic carbon analyser (Shimadzu TOC-VCPH, UK).

The mass of contaminants deposited on the membranes was calculating using a mass balance:

$$M_{Dep} = M_F - M_D - M_C \quad (4)$$

where,  $M_{Dep}$  is deposit,  $M_F$  feed,  $M_D$  diluate and  $M_C$  concentrate mass (mmol for H<sub>3</sub>BO<sub>3</sub>, F<sup>-</sup>, NO<sub>3</sub><sup>-</sup>), respectively.

## 2.4. Experimental Protocol

Concentrate and diluate pH was maintained constant during the experiments and adjusted by the addition of 1 mol/L HCl and/or NaOH in the range of pH 3-12. EC of both solutions was continuously monitored and samples were collected at the beginning and at 20 minute intervals for analyses of H<sub>3</sub>BO<sub>3</sub>, F<sup>-</sup>, NO<sub>3</sub><sup>-</sup>, UV-Vis absorbance and non-purgeable organic carbon (NPOC). After the completion of each experiment, cleaning solutions of 0.1 mol/L HCl, 0.1 mol/L NaOH and ultrapure water were circulated through the ED cell for 20 minutes each in order to remove any deposits. Samples taken from the cleaning solutions were analysed for UV-Vis absorbance and NPOC. After each set of OM experiments, the ED cell was dismantled and photographs were taken of the anion- and cation-exchange membranes.

Ion and EC removal ( $R_D$ , %) from the diluate was calculated using eqn (5):

$$R_D = \frac{(C_{Di}^0 - C_{Di}^T)}{C_{Di}^0} \times 100\% \quad (5)$$

where,  $C_{Di}^0$  is the initial diluate ion concentration or EC and  $C_{Di}^T$  is the diluate ion concentration or EC in the time period  $T$  (hours). Average ion and EC removal (%) was calculated along with standard deviation ( $\pm$  %). Note that ion removal includes deposit formation, while the flux of ions and EC ( $J_i$ , mmol/m<sup>2</sup>.h for ions and mS/cm/m<sup>2</sup>.h for EC) across the membranes was calculated using eqn (6):

$$J_i = \frac{(C_{Ci}^T - C_{Ci}^0)}{A_m T} \quad (6)$$

where,  $C_{Ci}^T$  (mmol for  $B(OH)_4^-$ ,  $F^-$  and  $NO_3^-$ ; mS/cm for EC) is concentrate mass (ions) in the concentrate in the time period  $T$ ,  $C_{Ci}^0$  is the initial mass within the concentrate and  $A_m$  is the membrane area ( $m^2$ ) used in the transport of the respective ion.

### 3. Results and Discussion

#### 3.1. Inorganic trace contaminant removal

As a first stage the removal of ions in the absence of OM was determined to establish a baseline. The removal of  $F^-$  from the diluate is shown in Figure 2A. The removal of  $F^-$  was independent of pH, which is due to the pH independence of  $F^-$  speciation [27].  $F^-$  ions removal was  $65.6 \pm 12.0 \%$ , while  $F^-$  flux was approximately  $10 \text{ mmol}/m^2 \cdot h$  (see Figure 3A).

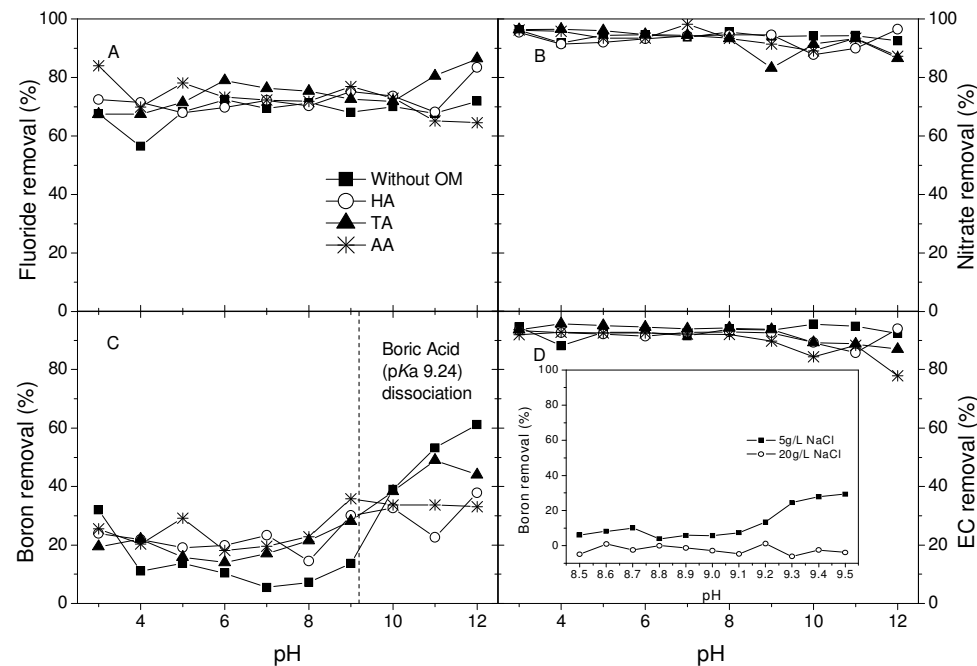


**Figure 2.** The removal of (A)  $F^-$ , (B)  $NO_3^-$ , (C)  $H_3BO_3$  and (D) EC (%) from the diluate as a function of solution pH (Initial concentrations 5 mg/L ( $F^-$ ), 100 mg/L ( $NO_3^-$ ), 10 mg/L ( $H_3BO_3$ ), 5 g/L NaCl; experiment duration 140min for each pH value).

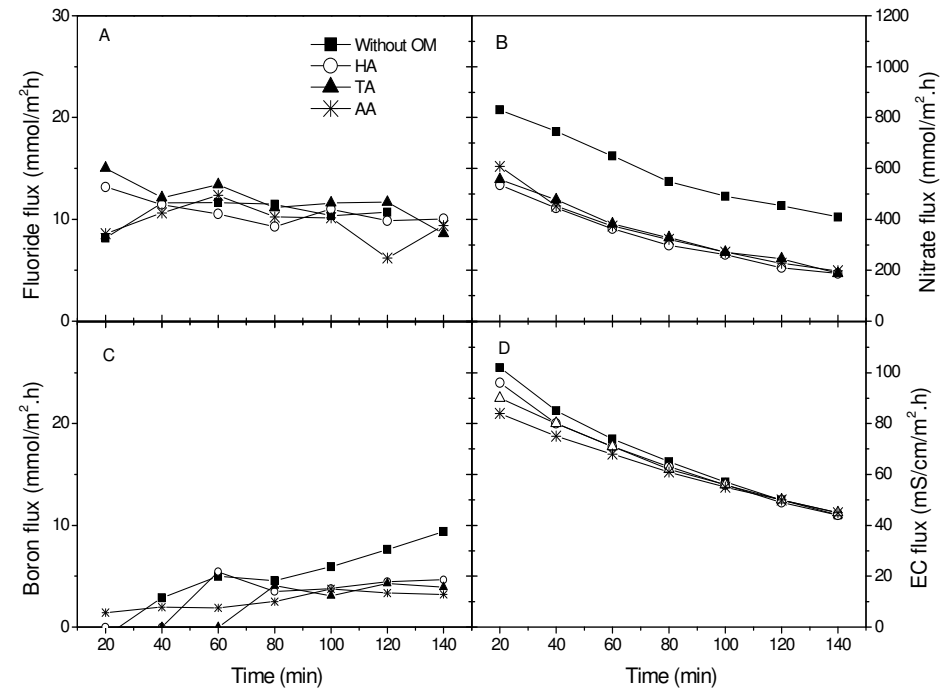


**Figure 3.** Flux of (A)  $F^-$  (B)  $NO_3^-$ , (C)  $B(OH)_4^-$  and (D) EC ( $\text{mmol}/m^2 \cdot h$ ) (Initial mass 2.1 mmol ( $F^-$ ), 57 mmol ( $NO_3^-$ ), 7.4 mmol ( $H_3BO_3$ ) (diluate and concentrate combined)).

Removal of  $NO_3^-$  is higher than that of  $F^-$  but equally pH independent (Figure 2B), again because  $NO_3^-$  speciation does not vary over the pH range studied [28]. The average removal of  $NO_3^-$  was  $94.1 \pm 1.3 \%$  while  $NO_3^-$  flux was significantly higher than for  $F^-$  and decreased gradually from 830 to 408  $\text{mmol}/m^2 \cdot h$  (Figure 3B).

$B(OH)_3$  does not dissociate at pH 3-8 and in consequence is not transported effectively through the AEM (see Figure 2C). Above pH 9 removal increases to 61.2 % at pH 12 due to  $B(OH)_3$  dissociation and speciation hence plays an important role. While Yazicigil *et al.* [13] determined that pH 9 was the optimal point for  $B(OH)_4^-$  removal, in this study it was only 13.7 % at pH 9.  $B(OH)_4^-$  flux is in the same order of magnitude as  $F^-$  but increased during experiments (see Figure 3C) which confirms the findings of Yazicigil *et al.* who attributed this to the increase in electrochemical potentials gradient between the diluate and concentrate (i.e. larger difference in salt concentration) [13]. The dissociation constant of  $B(OH)_3$  decreases with increasing NaCl concentration [29]. Further ED experiments were undertaken to examine this effect with a solution pH range between 8.5 and 9.5 (insert Figure 2D) at two feed NaCl concentrations of 5 and 20 g/L NaCl. In the 5 g/L experiment  $B(OH)_4^-$  removal ranged from 6.1 % at pH 8.5 to 29.4 % at pH 9.5.  $B(OH)_4^-$  was not removed over this pH range in the 20 g/L experiment presumably due to the higher concentration of competitive ions within the diluate. In consequence, no discernable shift in

the dissociation constant of  $B(OH)_3$  was observed. The results demonstrate however that NaCl concentration affects removal of other ions.

The ionic characteristics (Table 1) can be used to explain differences in the transport (removal and flux) of  $F^-$  and  $NO_3^-$  through the ion-exchange membranes. As no data was available on the hydrated radius of  $B(OH)_4^-$ , comparison of  $B(OH)_4^-$  removal and ionic characteristics is not discussed. Ions with smaller intrinsic crystal radii have higher hydration numbers, larger hydrated radii and hold their hydration shells more strongly [30], as illustrated in Figure 4. The crystal ionic radius of  $F^-$  is 0.116 nm compared with 0.179 nm for  $NO_3^-$ . The larger the crystal ionic radius the more diffuse the electric charge and the fewer water molecules surround the ion [31]. Therefore,  $NO_3^-$  ions are less hydrated than  $F^-$  ions may separate from its hydration layer [30] and transport through the ion-exchange membranes more easily.

The strength of hydration of  $F^-$  and  $NO_3^-$  is quantified by the Gibbs energy of hydration and the number of water molecules within their hydration shells.  $NO_3^-$  has a lower Gibbs free energy (-275 kJ/mol compared to -345 kJ/mol for  $F^-$ ). While it is to date not understood if water molecules separate from their ions during transport through ion-exchange membranes, it is hypothesised that separation is possible if the 'transport energy' is greater than the Gibbs free energy that bonds the hydrated shell to the ion.

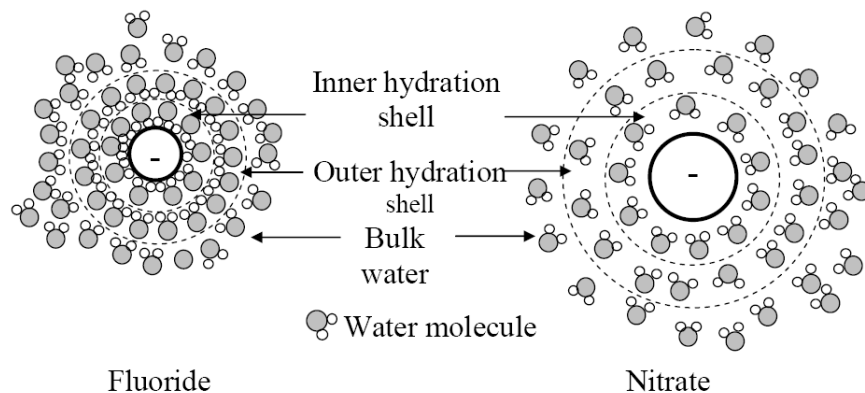


**Figure 4.** Schematic representation of hydration shells around  $F^-$  and  $NO_3^-$  ions (adapted from [35]).

Ion mobility ionic permeabilities [32] further influence transport through ion-exchange membranes. The ionic mobility of  $NO_3^-$  in solution ( $7.4 \times 10^{-8} \text{ m}^2/\text{sV}$ ) solution is greater than the ionic mobility of  $F^-$  ( $5.7 \times 10^{-8} \text{ m}^2/\text{sV}$ ) [33]. The current passing through an ionic solution in ED and the resultant transport of ions is related to the conductivity of the ionic solutions. The ion equivalent conductivity of  $NO_3^-$  ( $71.5 \text{ cm}^2/\Omega.\text{equiv}$ ) is also greater than that of  $F^-$  ( $55.4 \text{ cm}^2/\Omega.\text{equiv}$ ), all factors contributing to higher flux of  $NO_3^-$  than  $F^-$ . To confirm those results independent of their concentration, an experiment with the same initial mass concentration for boron,  $F^-$  and  $NO_3^-$  (10 mg/L at pH 10) was carried out. The removal of  $NO_3^-$  was 95.3 % compared with 76.2 % for  $F^-$ , further indicating that  $NO_3^-$  with the smaller hydrated radius is removed more efficiently than  $F^-$  with the larger hydrated radius.

### 3.2. Organic matter removal

Figure 5 shows the removal of OM as a function of solution pH in diluate and concentrate. The fact that OM is removed from both compartments indicates that this removal is a deposition on the membrane rather than transport through the membrane. However, staining of the membranes indicates that membrane penetration also occurs. Removal of AA from the diluate is low with an average of  $9.2 \pm 1.6 \%$  and independent of pH given its negative charge at pH 3-12. The removal of HA and TA from the diluate is higher with an average removal of  $19.1 \pm 3.7 \%$  and  $19.8 \pm 9.5 \%$ , respectively. While HA removal is pH independent, the removal of TA increased with pH to 44.3 % at pH 12 due to its increasing negative charge. Removal of OM from the concentrate was less than from the diluate due to electrostatic repulsion with the negatively charged functional groups in the CEMs adjacent to the concentrate compartment. This confirms the results of Park et al. who found that deposits occur mostly on the diluate side of AEM membranes.

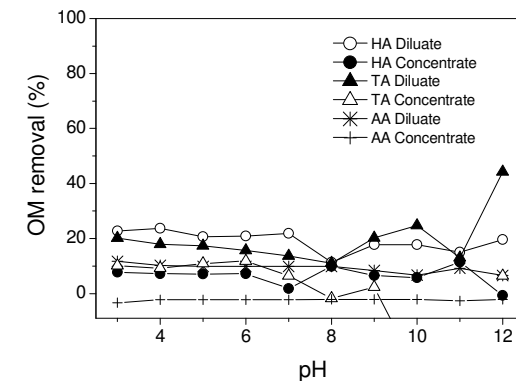


**Figure 5.** Organic matter (OM) removal as a function of solution pH (Initial OM concentration 12.5 mgC/L).

### 3.3. Effect of organic matter on inorganic trace contaminant removal

Organic matter (OM) deposits on the membranes and interacts with inorganic contaminants. The removal of  $F^-$  was greater in the presence of OM (Figure 2A), which can be attributed to the binding of  $F^-$  to the OM [16]. The average percentage of  $F^-$  ions removed with TA was  $74.8 \pm 6.0 \%$ , followed by AA and HA with  $72.9 \pm 5.8 \%$  and  $72.5 \pm 4.5 \%$  respectively. The flux of  $F^-$  was reduced in the presence of OM. The final flux (after 140 minutes) was  $10.0 \text{ mmol}/\text{m}^2.\text{h}$ ,  $8.6 \text{ mmol}/\text{m}^2.\text{h}$  and  $9.4 \text{ mmol}/\text{m}^2.\text{h}$  with HA, TA and AA, respectively compared to  $10.7 \text{ mmol}/\text{m}^2.\text{h}$  in the absence of OM. Combined increase in removal and reduced flux indicates  $F^-$  membrane deposition.

No significant difference in  $\text{NO}_3^-$  due to OM; HA ( $91.9 \pm 3.5 \%$ ), TA ( $91.4 \pm 4.9 \%$ ) and AA ( $92.6 \pm 0.8 \%$ ) removal was observed. For experiments with TA,  $\text{NO}_3^-$  removal was highest under acidic-neutral pH conditions (95.2 - 93.2 % at pH 3 - 7). In HA experiments,  $\text{NO}_3^-$  removal was pH independent while the flux of  $\text{NO}_3^-$  (Figure 3B) was reduced in the presence of OM. This again demonstrated some degree of membrane deposition.

The presence of OM also enhanced boron removal between pH 3 and 8 (Figure 2C) while above pH 9, the removal of  $\text{B}(\text{OH})_4^-$  in the presence of OM was lower.  $\text{B}(\text{OH})_4^-$  flux at high pH was lower in the presence of OM (Figure 3C), and again results indicate  $\text{B}(\text{OH})_4^-$ -OM complexation and  $\text{B}(\text{OH})_4^-$  membrane deposition.

### 3.4. Inorganic trace contaminant membrane deposition

The deposit formation can be quantified using mass balance. The mass of  $\text{F}^-$  deposited on the membranes is shown in Figure 6A, with negligible deposition in experiments without OM. In the presence of OM the mass of  $\text{F}^-$  deposited was between 0.1 and 0.6 mmol (4.7 and 28.8 % initial mass); with a greater amount deposited with HA and TA. HA contains voids which can trap inorganic compounds [34] and binding of  $\text{F}^-$  has been shown to be pH dependent [16]. Hayes [16] studied the binding of  $\text{F}^-$  to HA as a function of solution pH (5.0 - 6.6) and in this narrow pH range  $\text{F}^-$  was being trapped within the large structure of HA rather than bound to a particular functional group. As solution pH increases HA deprotonates and the negative charge on the carboxylates repels the  $\text{F}^-$  ion. This phenomenon was not observed in this current study due to the fact that the adsorption of  $\text{F}^-$  in ED would be governed by several other factors (e.g. presence of other contaminants).

The mass of  $\text{NO}_3^-$  deposited on the membranes was greater in experiments with OM (Figure 6B) with values of between 4.6 and 13.8 mmol (8.1 and 24.2 % initial mass). Contrary to the negative charge of HA above pH 5 (Table 2) the mass of  $\text{NO}_3^-$  adsorbed to the membranes in the presence of HA increased above pH 5. Adsorption of  $\text{NO}_3^-$  in experiments with TA was independent of pH. In the presence of AA, the mass of  $\text{NO}_3^-$  adsorbed was lower at pH 6 - 8 because repulsion between the negatively charged AA and  $\text{NO}_3^-$  would be expected.

The mass of  $\text{B}(\text{OH})_4^-$  deposited on the membranes is greater in experiments with OM (Figure 6C) with values of between 0.3 and 1.4 mmol (4.0 and 19.0 % initial mass). Removal of  $\text{B}(\text{OH})_3$  between pH 3 and 8 (Figure 2C) may be the result of  $\text{B}(\text{OH})_3$  complexation with polar organic compounds [35], such as HA. Schmitt-Kopplin *et al.* [36] postulated that  $\text{B}(\text{OH})_3$  binds to carboxylate groups ( $\text{COO}^-$ ) within HA where it forms a transient hydrogen bonded structure with the HA. A schematic of this complexation mechanism is shown in Figure 7. Due to the transport direction of the negatively charged HA,  $\text{B}(\text{OH})_4^-$  is deposited on the AEMs.

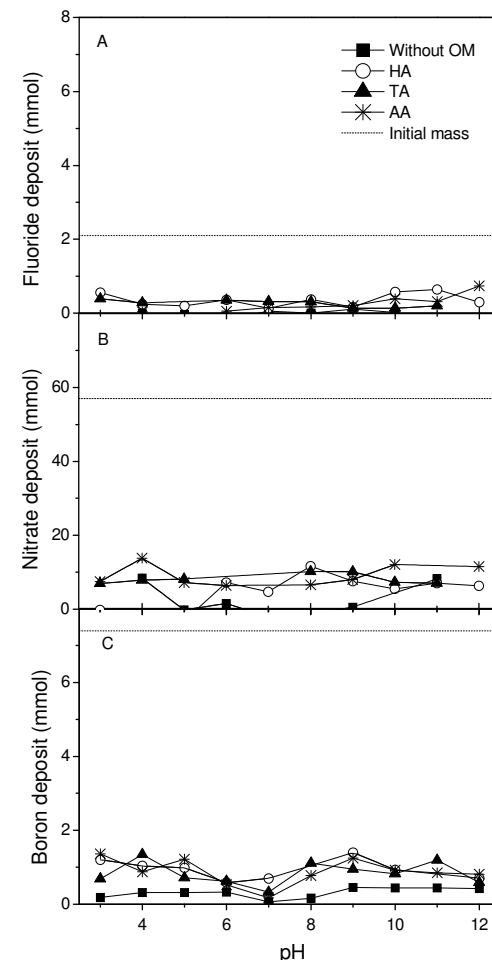


**Figure 6.** Membrane deposit of (A)  $\text{F}^-$  (B)  $\text{NO}_3^-$  and (C)  $\text{B}(\text{OH})_4^-$  as a function of pH. (Initial mass 2.1 mmol ( $\text{F}^-$ ), 57 mmol ( $\text{NO}_3^-$ ), 7.4 mmol ( $\text{H}_3\text{BO}_3$ ) (diluate and concentrate combined)).

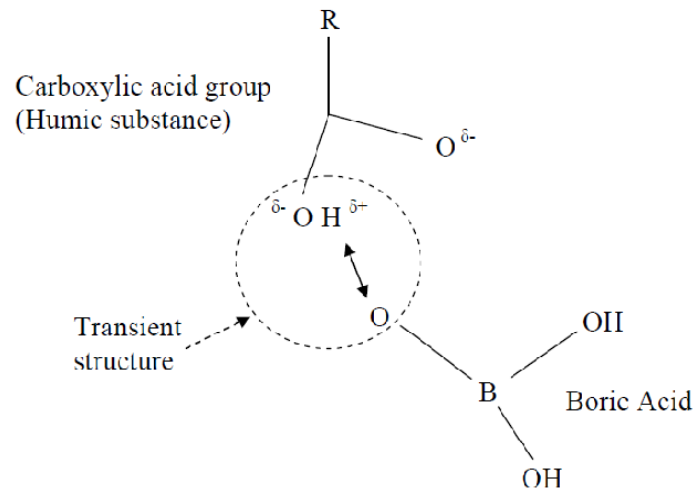


Figure 7. Schematic of  $B(OH)_3$  complexation with humic substances.

### 3.5. Organic matter membrane deposition

UV-Vis and NPOC measurements showed a decrease in OM within the ED system over the duration of each experiment. The reduction of OM in both diluate and concentrate indicates that the OM is deposited. Figure 8 shows that the mass of OM (mgC) deposited on the AEMs was greater than the mass deposited on the CEMs, which confirms results Lee *et al.* [20]. The negatively charged HA deposits more readily on the positively charged AEMs in experiments with a higher solution pH. However, Park *et al.* [37] showed that HA has a negative zeta potential in a wide pH range, so that it can foul AEMs in almost the entire pH range. In this study the amount of HA deposited on the AEMs showed a slight decrease with increasing solution pH (from pH 6) (Figure 8A) which cannot be explained by repulsive forces. The macromolecular structures of humic substances influences the properties and affinities of these materials [38]. According to Chen and Schnitzer [39], humic substances behave like uncharged (spherical) polymers at very low pH whereas at high pH, they exhibit polyelectrolytic character of linear shape. Lee *et al.* [17] postulated that the fouling of an AEM is related more to the properties of the foulant (humate) than the electrostatic force between the foulant and the membrane.

Unlike HA, the mass of TA deposited on the AEM was pH independent (Figure 8B), with an exception (decrease) at neutral pH. As large molecular weight organics have more difficulty in permeating the AEMs [37], TA, with its lower molecular weight, has increased potential for transportation through the AEM compared to HA.

The mass of AA deposited on the AEMs was lower than HA and TA over the studied pH range (Figure 8C). Avaltroni *et al.* [26] found that the structure of AA follows three pH dependent trends (1) increased aggregation below pH 4 due to a decrease in charge density, (2) molecular expansion between pH 4 and 8 and (3) dissociation above pH 8. The variability seen in the mass above pH 8 could be attributed to AA dissociation.

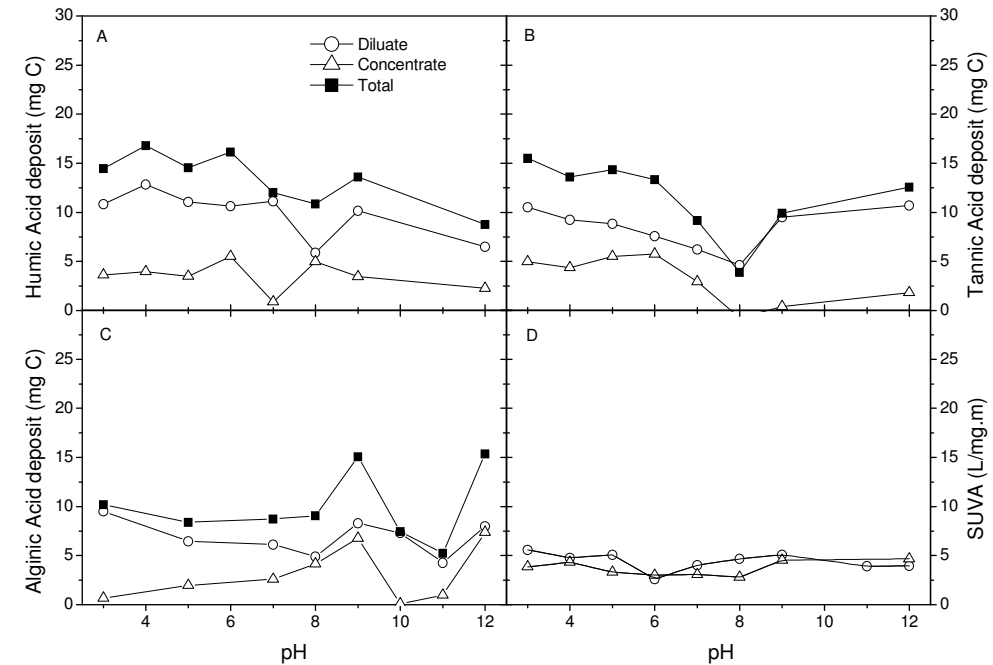


Figure 8: Membrane deposit of (A) Humic, (B) Tannic and (C) Alginic acids and (D) SUVA ( $L/mg.m$ ) for HA as a function of pH (Initial mass of OM 100 mgC).

The AEM surface in contact with the diluate showed visible fouling with HA and TA. This fouling was not reversed by chemical cleaning indicative of strong binding of the OM to the AEM functional groups and penetration into the membrane. The observed colour change was more pronounced on the area of membranes in contact with ED cell inlets. The fouling of the AEMs was also accompanied by visible swelling. The hydrophobic and hydrophilic acids contained in OM cannot pass through the membranes due to their high molecular weight and it is thought that a fraction of the OM is transported through the membranes as a result of their negative charge density and molecular structure [17, 18]. The surface of the CEMs in contact with both the concentrate and diluate presented little visible evidence of fouling, due to electrostatic repulsion of the negatively charged functional groups within the CEM.

SUVA ( $L/mg.m$ ) values for HA experiments are shown in Figure 8D. SUVA is used as an indicator for the aromatic content of carbon within a water sample [40]. SUVA values in the diluate and concentrate for the HA experiments were pH and time independent with a values between 2.6 and 5.6  $L/mg.m$ . Shin *et al.* [41] stated that the non-aromatic (aliphatic nature) fractions of HA have a larger molecular size in comparison to the aromatic and carboxylate groups of smaller size

fractions. Results from this study, therefore, indicate that ED does not separate the aromatic and non-aromatic fractions of HA.

### 3.6. ED parameters and performance

An increase in ED stack resistance (see Eqn (2)) was observed at the beginning of the ED process in all experiments as a result of ion depletion within the diluate and membrane boundary layer. An increase in resistance observed at the end of the ED experiments without OM is attributed to the higher demineralization rate in the diluate solution. ED stack resistance as a function of solution pH is shown in Figure 9.

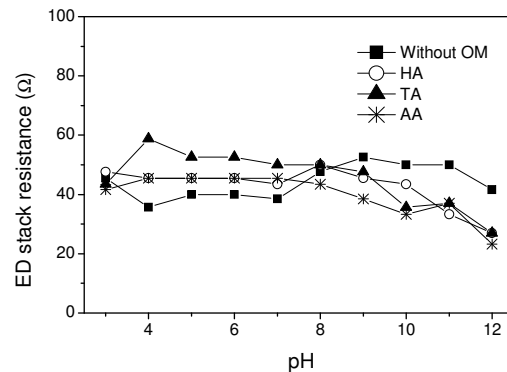


Figure 9. ED stack resistance as a function of solution pH.

The deposition of inorganic trace contaminants and OM on the membranes has implications for ED performance. OM deposition as a foulant layer on and/or inside the membranes increases the resistance at the membrane surface [19, 42]. Between pH 3 and 8 the average stack resistances were indeed greater in the presence of OM; HA ( $46.3 \pm 2.2 \Omega$ ), TA ( $51.3 \pm 5.0 \Omega$ ) and AA ( $44.5 \pm 1.6 \Omega$ ), due to enhanced OM deposition within this pH range (Figure 8). Above pH 8, resistance decreased due to decreased OM membrane deposition.

The performance of the ED process can also be evaluated by the removal of EC (Figure 2D). The average percentage of EC removed without OM was  $93.0 \pm 2.1 \%$  compared with  $91.7 \pm 2.5 \%$ ,  $92.6 \pm 3.0 \%$  and  $89.4 \pm 4.8 \%$  with HA, TA and AA respectively. The presence of OM on the membranes did not significantly lower EC removal. It is possible the OM was loosely packed on the AEM still allowing for the migration of salt ions through the membrane; though at a slightly decreased initial flux (Figure 4D).

### 4. Conclusions

The purpose of this study was to understand the impact of OM on inorganic contaminant removal. The removal of the contaminants followed the order  $\text{NO}_3^- > \text{F}^- > \text{B}(\text{OH})_4^-$ . The hydrated radius and subsequent strength of hydration shells is a parameter that plays a significant role in the transport of the ions during ED; as  $\text{NO}_3^-$  with a smaller hydrated ionic radii and subsequent weaker hydration shell was removed more effectively than  $\text{F}^-$  with a larger hydrated ionic radii and stronger hydration shell. The transport of  $\text{B}(\text{OH})_4^-$  in ED was solution pH and hence speciation dependent with increased removal at high pH.

The removal of the inorganic contaminants was enhanced by the presence of OM while the flux decreased indicating mutual dependence of inorganic and organic contaminants in ED. The mechanism for this involves the possible territorial binding and/or complexation of the inorganic contaminants to the negatively charged OM and the subsequent OM deposition on the positively charged AEMs. This membrane deposition led to an increase in stack resistance and a slight reduction in initial EC flux. It is important to study the behaviour of these trace contaminants with OM to better understand the feasibility and applicability of ED for the treatment of real waters.

### 5. Acknowledgements

This work was initially funded through the Australian Research Council (ARC) Linkage Project LP0454254 in collaboration with Brisbane Water along with the ARC Discovery Project DP0559878. The authors thank Eurodia (Germany and France) for the provision of membranes for this project and Berghof (Germany) for the donation of the ED stack. Wytze Meindersma (Eindhoven University of Technology, Netherlands) and Bart van der Bruggen (University of Leuven, Belgium) are acknowledged for helpful discussions. Steffen Zuleeg (EAWAG, Switzerland) and Johannes Fritsch (University of Applied Sciences, Ravensburg-Weingarten, Germany) for help with limiting current density issues. The authors also thank Peter Anderson and Alan Simm (University of Edinburgh, UK) for boron analysis and discussions on boron chemistry and laboratory support, respectively.

### References

- [1] WHO, Guidelines for Drinking Water Quality, World Health Organization, 2006.
- [2] R. Abu, K. Alsokhny, Geochemical assessment of groundwater contamination with special emphasis on fluoride concentration, North Jordan, *Chemie der Erde - Geochem.* 64 (2004) 171.
- [3] N. Tamer, B.K. Köroğlu, C. Arslan, M. Akdoğan, M. Köroğlu, H. Çam, M. Yildiz, Osteosclerosis due to endemic fluorosis, *Sci. Total Environ.* 373 (2007) 43.
- [4] M. Zeni, R. Riveros, K. Melo, R. Primieri, S. Lorenzini, Study on fluoride reduction in artesian well-water from electro dialysis process, *Desalination.* 185 (2005) 241.
- [5] A. Elmidaoui, F. Elhannouni, M. Taky, L. Chay, M.A. Menkouchi Sahli, L. Echihabi, M. Hafsi, Optimization of nitrate removal operation from ground water by electro dialysis, *Sep. Purif. Technol.* 29 (2002) 235.
- [6] Council Directive 98/83/EC of 3 November 1998 on the quality of water intended for human consumption, *Official Journal L* 330, European Union, 1998, pp. 32-54.
- [7] NHMRC, Australian Drinking Water Guidelines, National Health and Medical Research Council, Canberra, 2004.
- [8] K. Kesore, F. Janowski, V.A. Shaposhnik, Highly effective electro dialysis for selective elimination of nitrates from drinking water, *J. Membr. Sci.* 127 (1997) 17.
- [9] J.M. Ortiz, J.A. Sotoca, E. Exposito, F. Gallud, V. Garcia-Garcia, V. Montiel, A. Aldaz, Brackish water desalination by electro dialysis: batch recirculation operation modeling, *J. Membr. Sci.* 252 (2005) 65.
- [10] M. Turek, P. Dydo, J. Trojanowska, B. Bandura, Electro dialytic treatment of boron-containing wastewater, *Desalination.* 205 (2007) 185.
- [11] L. Melnyk, V. Goncharuk, I. Butnyk, E. Tsapiuk, Boron removal from natural and wastewaters using combined sorption/membrane process, *Desalination.* 185 (2005) 147.
- [12] L. Melnik, O. Vysotskaja, B. Kornilovich, Boron behavior during desalination of sea and underground water by electro dialysis, *Desalination.* 124 (1999) 125.
- [13] Z. Yazicigil, Y. Oztekin, Boron removal by electro dialysis with anion-exchange membranes, *Desalination.* 190 (2006) 71.
- [14] J.A. Dean, Lange's handbook of chemistry, McGraw-Hill, New York, 1999.



- [15] F.H. Frimmel, Characterization of natural organic matter as major constituents in aquatic systems, *J. Contam. Hydrol.* 35 (1998) 201.
- [16] D. Hayes, J. Carter, T.J. Manning, Fluoride binding to humic acid, *J. Radioanal. Nucl. Chem. Lett.* 201 (1995) 135.
- [17] H.J. Lee, D.H. Kim, J. Cho, S.H. Moon, Characterization of anion exchange membranes with natural organic matter (NOM) during electro dialysis, *Desalination*. 151 (2002) 43.
- [18] D.H. Kim, S.H. Moon, J. Cho, Investigation of the adsorption and transport of natural organic matter (NOM) in ion-exchange membranes, *Desalination*. 151 (2002) 11.
- [19] J.S. Park, J.H. Choi, K.H. Yeon, S.H. Moon, An approach to fouling characterization of an ion-exchange membrane using current-voltage relation and electrical impedance spectroscopy, *J. Colloid Interface Sci.* 294 (2006) 129.
- [20] H.J. Lee, J.H. Choi, J. Cho, S.H. Moon, Characterization of anion exchange membranes fouled with humate during electro dialysis, *J. Membr. Sci.* 203 (2002) 115.
- [21] A. Kopal, U. Ogutveren, Removal of nitrate from water by electroreduction and electrocoagulation, *J. Hazard. Mater.* 89 (2002) 83.
- [22] Y.P. Chin, G. Aiken, E. O'Loughlin, Molecular Weight, Polydispersity, and Spectroscopic Properties of Aquatic Humic Substances, *Environ. Sci. Technol.* 28 (1994) 1853.
- [23] T. Shutava, M. Prouty, pH responsive decomposable layer-by-layer nanofilms and capsules on the basis of tannic acid, *Macromolecules*. 38 (2005) 2850.
- [24] J.H. An, S. Dultz, Adsorption of tannic acid on chitosan-montmorillonite as a function of pH and surface charge properties, *Appl. Clay Sci.* 36 (2007) 256.
- [25] T. Coradin, J. Livage, Synthesis and characterization of alginate/silica biocomposites, *J. Sol-Gel Sci. Technol.* 26 (2003) 1165.
- [26] F. Avaltroni, M. Seijo, S. Ulrich, S. Stoll, K.J. Wilkinson, Conformational Changes and Aggregation of Alginic Acid as Determined By Fluorescence Correlation Spectroscopy, *Biomacromolecules*. 8 (2007) 106.
- [27] L.A. Richards, B.S. Richards, H.M.A. Rossiter, A.I. Schäfer, Impact of speciation on fluoride, arsenic and magnesium retention by nanofiltration/reverse osmosis in remote australian communities, *Desalination*. Accepted (2009).
- [28] L.A. Richards, B.S. Richards, H.M.A. Rossiter, A.I. Schäfer, Impact of speciation on fluoride, arsenic and magnesium retention by nanofiltration/reverse osmosis in remote australian communities, *Desalination*. In press (2008).
- [29] B.B. Owen, E.J. King, The Effect of Sodium Chloride upon the Ionization of Boric Acid at Various Temperatures, *J. Amer. Chem. Soc.* 65 (1943) 1612.
- [30] B. Tansel, J. Sager, T. Rector, J. Garland, R.F. Strayer, L. Levine, M. Roberts, M. Hummerick, J. Bauer, Significance of hydrated radius and hydration shells on ionic permeability during nanofiltration in dead end cross flow modes, *Sep. Purif. Technol.* 51 (2006) 40.
- [31] A.G. Volkov, S. Paula, D.W. Deamer, Two mechanisms of permeation of small neutral molecules and hydrated ions across phospholipid bilayers, *Bioelectrochem. Bioenerg.* 42 (1997) 153.
- [32] H. Strathmann, Ion-exchange membrane separation processes, Elsevier, Amsterdam, Netherlands, 2004.
- [33] P.W. Atkins, Physical chemistry, Oxford University Press, Oxford, 1990.
- [34] H.R. Schulten, M. Schnitzer, Three-dimensional models for humic acids and soil organic matter, *Naturwissenschaften*. 82 (1995) 487.
- [35] E. Chauveheid, M. Denis, The boron-organic carbon correlation in water, *Water Research*. 38 (2004) 1663-1668.
- [36] P. Schmitt-Kopplin, N. Hertkorn, A.W. Garrison, D. Freitag, A. Kettrup, Influence of Borate Buffers on the Electrophoretic Behavior of Humic Substances in Capillary Zone Electrophoresis, *Anal. Chem.* 70 (1998) 3798.
- [37] J.S. Park, H.J. Lee, S.J.G. Choi, K.E., J. Cho, S.H. Moon, Fouling mitigation of anion exchange membrane by zeta potential control, *J. Colloid Interface Sci.* 259 (2003) 293.
- [38] K. Ghosh, M. Schnitzer, Macromolecular structures of humic substances, *Soil Science*. 129 (1980) 266.
- [39] Y. Chen, M. Schnitzer, Viscosity measurements on soil humic substances, *Soil Sci. Soc. Am. J.* 40 (1976) 866.
- [40] J.P. Croué, D. Violleau, C. Bodaire, B. Legube, Removal of hydrophobic and hydrophilic constituents by anion exchange resin, *Water Sci. Technol.* 40 (1999) 207.
- [41] H.S. Shin, J.M. Monsallier, G.R. Choppin, Spectroscopic and chemical characterizations of molecular size fractionated humic acid, *Talanta*. 50 (1999) 641.
- [42] V. Lindstrand, G. Sundstrom, A.S. Jonsson, Fouling of electro dialysis membranes by organic substances, *Desalination*. 128 (2000) 91.
- [43] M.Y. Kiriukhin, K.D. Collins, Dynamic hydration numbers for biological important ions, *Biophys. Chem.* 99 (2002) 155.
- [44] K.D. Collins, Sticky ions in biological systems, *Proc. Natl. Acad. Sci. US.* 92 (1995) 5553.
- [45] L. Pauling, The nature of the chemical bond and the structure of molecules and crystals: An introduction to modern structural chemistry, Cornell University Press, New York, 1960.
- [46] H. Corti, R. Crovetto, R. Fernandez-Prini, Mobilities and ion-pairing in LiB(OH)<sub>4</sub> and NaB(OH)<sub>4</sub> aqueous solutions. A conductivity study, *J. Sol. Chem.* 9 (1980) 617.
- [47] Y. Marcus, Thermodynamics of solvation of ions Part 5.- Gibbs free energy of hydration at 298.15 K, *J. Chem. Soc. Faraday Trans.* 87 (1991) 2995.
- [48] R.A. Robinson, R.H. Stokes, Electrolyte solutions, Butterworths, London, 1970.
- [49] Y.P. Chin, G. Aiken, K.M. Danielsen, Binding of pyrene to aquatic and commercial humic substances: The role of molecular weight and aromaticity, *Environ. Sci. Technol.* 31 (1997) 1630.
- [50] M. Fukushima, S. Tanaka, H. Nakamura, S. Ito, Acid-base characterization of molecular weight fractionated humic acid, *Talanta*. 43 (1996) 383.
- [51] G.R. Choppin, P.M. Shanbhag, Binding of calcium by humic acid, *J. Inorg. Nucl. Chem.* 43 (1981) 921.
- [52] M. Terashima, M. Fukushima, S. Tanaka, Influence of pH on the surface activity of humic acid: micelle-like aggregate formation and interfacial adsorption, *Colloids Surf., A.* 247 (2004) 77.
- [53] H.R. Schulten, A chemical structure for Humic Acid. Pyrolysis-gas chromatography/mass spectrometry and pyrolysis-soft ionization mass spectrometry evidence, in: N. Senesi, T.M. Miano, (Eds), Humic substances in the global environment and implications on human health, Elsevier Science, 1994, pp. 43-56.